Journal of the Korean Nuclear Society
Volume 36, Number 1, pp.104~111, February, 2004

Measurement of Melting Temperatures of UO_2, $(U,Gd)O_2$ and $(U,Er)O_2$ Fuels

Ki Won Kang, Jae Ho Yang, Keon Sik Kim, Jong Hun Kim, Young Woo Lee, and Kun Woo Song
Korea Atomic Energy Research Institute
150 Dukjindong, Yuseong-gu, Daejeon, 305-353, Korea
kwkang@kaeri.re.kr

(Received September 5, 2003)

Abstract

The melting temperatures of UO_2, UO_2-6wt%Gd_2O_3, UO_2-12wt%Gd_2O_3, UO_2-2wt%Er_2O_3, and UO_2-4wt%Er_2O_3 fuels were measured. Fuel materials were loaded in a tungsten capsule of which shape met the black body condition. The melting temperature was measured by the thermal arrest method during heating of the capsule in an induction furnace. The measured melting temperature of UO_2 fuel was 2815±20℃. The solidus and liquidus temperatures of UO_2-Gd_2O_3 and UO_2-Er_2O_3 had also been measured, and it was observed that the solidus temperatures of them were lower than the liquidus temperature by 15~25℃.

Measured melting temperatures of UO_2, UO_2-Gd_2O_3 and UO_2-Er_2O_3 fuels were as follows:

Material	Melting temperature(℃)	
	T_S	T_L
UO_2	2815±20	
UO_2-6wt%Gd_2O_3	2763±25	2791±20
UO_2-12wt%Gd_2O_3	2779±25	2795±20
UO_2-2wt%Er_2O_3	2800±25	2816±20
UO_2-4wt%Er_2O_3	2798±25	2811±20

Key Words : melting temperature, thermal arrest method, UO_2, UO_2-Gd_2O_3, UO_2-Er_2O_3

1. Introduction

Various types of oxides are currently used as fuel materials in nuclear reactors; UO_2, $(U,Gd)O_2$, $(U,Pu)O_2$, and $(U,Er)O_2$. The melting temperature of nuclear fuel is one of the most important properties for estimating the behavior of nuclear fuel during both normal operation and postulated accident conditions. The melting temperature have generally been measured by one of the two methods; namely filament technique [1-2] and thermal arrest method [3].

The filament technique used a V-shaped tungsten filament (crucible) which is directly heated by

electrical resistance, and the fuel material put on the filament is observed through a window during heating. The melting temperature is determined at which fuel material lost its integrity. As the melting temperature measured by the filament technique is severely fluctuated, it is no longer used in the measurement of the melting temperature.

The thermal arrest method is based on the fact that fuel material absorbs heat of fusion on the transition from solid to liquid. The melting temperature can be experimentally determined by the temperature, at which the increasing temperature is arrested during the heating of fuel. This method requires somewhat difficult techniques of heating fuel with an electrical induction furnace and measuring very high temperatures with a pyrometer. However, this method enables us to measure the melting temperature with better accuracy and reproducibility than the filament technique.

The melting temperature of UO_2 fuel is relatively well known for both unirradiated[3-6] and irradiated fuel[2, 7-9]. $(U,Gd)O_2$ fuel has been increasingly used, but several data are known about its melting temperature[10-11]. $(U,Er)O_2$ fuel is one of the burnable absorber fuels for longer fuel cycle, but its melting temperature is not known in open literature. So more data for the melting temperatures of $(U,Gd)O_2$ and $(U,Er)O_2$ fuels are needed.

This paper describes an equipment developed for the melting temperature measurement by the thermal arrest method and the experimental results of the melting temperature of UO_2, $(U,Gd)O_2$, and $(U,Er)O_2$ fuels.

2. Apparatus Development

An apparatus was developed for melting fuels and measuring temperature. Fig. 1 shows a schematic diagram of the equipment consisting of

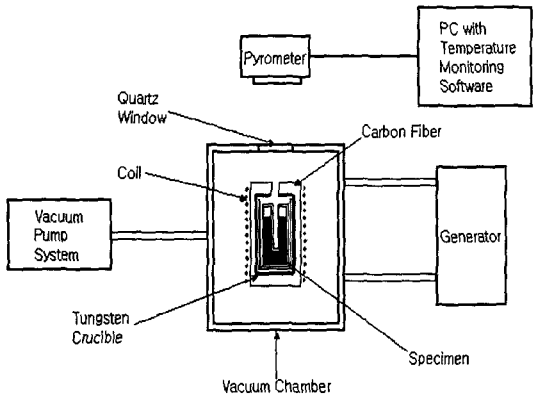

Fig. 1. Schematic Diagram of an Apparatus for Measuring the Melting Temperature

induction generator, vacuum chamber, vacuum pump, pyrometer, and computer. The vacuum chamber includes tungsten capsule, tungsten susceptor, carbon fiber insulator, and induction coil in it. The capsule is a cylinder with 13mm diameter and 38mm height, and a special long hole, not through-hole, with 5mm diameter and 30mm height is made in the central position of the capsule. This long hole can provide the black body condition for measuring temperature.

The carbon fiber was used to insulate outside heat flow. Carbon tends to combine with tungsten to produce tungsten carbide, which has the melting point of about 2776℃[12]. Once this reaction occurs, a further heating above the melting temperature of tungsten carbide is found very difficult because the melting process continuously consumes thermal input. To avoid this reaction the inner side of carbon fiber was covered with tantalum foil.

The induction generator has a frequency of 10 kHz and a capacity of 20 kW. The temperature of fuel was measured at the black body hole by a pyrometer mounted on the X-Y stage. This X-Y stage gave us conveniences when the measuring point was being concentrated on an accurate position of the hole.

3. Experimental Procedures

Fuel materials used in the melting experiment were UO_2, UO_2-(6,12)wt%Gd_2O_3 and UO_2-(2,4)wt% Er_2O_3 fuels. The UO_2 powder used in this work was produced through the ADU(Ammonium Di-Uranate) process. The four powder mixtures, UO_2-(6,12)wt%Gd_2O_3 and UO_2-(2,4)wt%Er_2O_3, were prepared by mixing in a tumbling mixer for 1 h, respectively. The powder mixtures were ball milled for 24 h in a jar containing zirconia balls and alcohol and then dried in air. The prepared powders were pressed at 3 ton/㎠ into compacts. The UO_2-(6,12)wt%Gd_2O_3 and UO_2-(2,4)wt%Er_2O_3 pellets had been produced by sintering at 1730℃ for 4 h in hydrogen-3%steam gas. The UO_2 pellets were fabricated by sintering at 1700℃ for 4 h in hydrogen gas. For the measurement specimens, fuel materials were fragments from sintered pellets. About 10g of each fuel was loaded in the tungsten capsule, which was evacuated down to 10^{-2} torr, and then the capsule was filled with helium. After seal-welding, a helium leak test was performed to confirm that the capsule has no leak.

The capsule, tungsten susceptor, tantalum foil and carbon fiber were placed within the induction coil, in that order. The vacuum chamber was evacuated below 10^{-4} torr. The induction generator was manually operated; the power input for heating the capsule was increased step by step with a time interval. This heating method is shown schematically in Fig. 2(a), and it is very similar to that of Adamson et al. [13].

When the power input jumps to a higher step, the temperature rises rapidly and then rises slowly, and finally the temperature levels off [see Fig. 2(b)]. While the power jump is being repeated, the temperature is increased with a similar profile. An empty capsule was heated several times, for which the temperature profile was obtained as shown in Fig. 2(b).

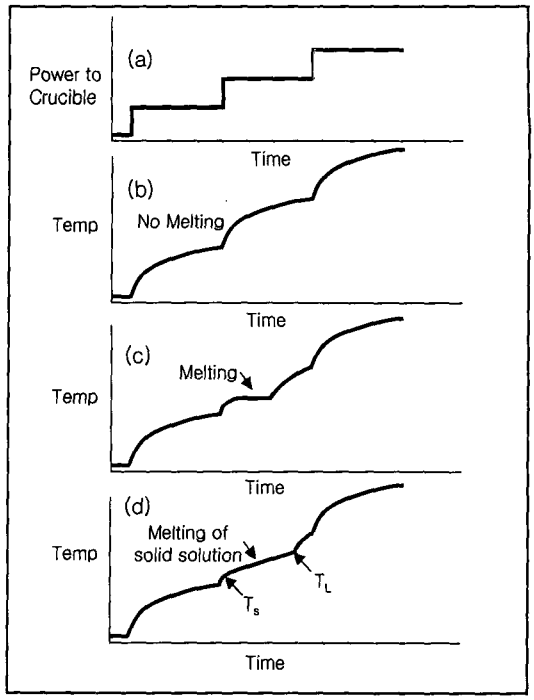

Fig. 2. Temperature (power)-time Curves Showing Thermal Arrest Methods for Stepwise Heating

Fig. 2(c) shows the change in temperature profile in accordance with the melting of fuel. If the melting occurs in one step, the temperature rising is arrested for some time and then restarts. The melting point was determined by the temperature at which the rising temperature remains temporarily arrested.

If the melting of solid solution occurs in a certain range of temperature, the temperature-time profile changes like Fig. 2(d). The melting starts at the solidus temperature(T_S) and ends at the liquidus temperature(T_L). The temperature increases with lower rates between the T_S and T_L but does not remain constant, and then the temperature increases with a high rate.

The temperature of capsule was continuously monitored through a pyrometer and recorded in a

time interval of 0.2 sec by a computer. The pyrometer was focused on the black body hole of the capsule. The emissivity (ϵ) of the pyrometer was chosen to be 0.9 in order to correct for an optical loss from a quartz window of the vacuum chamber. The temperature obtained by the pyrometer was calibrated against the known melting temperatures of materials such as MgO, ZrO_2 and Er_2O_3. These materials were melted in the same way as the fuel materials.

With one capsule containing a fuel, we measured the melting temperature at least 3 times by repeating the heating and cooling around the melting temperature without capsule failure. In this case the difference among the measured melting temperatures was in the range of ±10℃. When the same material was melted with new capsules and new alignment of pyrometer, the melting temperature was further changed. But the differences of all the measured melting temperatures of the same material were in the range of ±20℃. So the uncertainty of the melting temperature which might be associated with this equipment and method is believed to be ±20℃. This uncertainty does not have any statistical significance but simply represents a conservative estimate of the maximum error derived from experimental error and instrumental bias. The solidus temperature is found to be difficult to read from the temperature-time plot because of a blunt change in the plot. The uncertainty associated with the solidus temperature is considered to be ± 25℃. The solidus and liquidus temperatures were determined by averaging three measurements.

4. Results and Discussion

4.1. Melting Temperature of UO_2

A typical temperature-time profile for the determination of UO_2 melting temperature is shown in Fig. 3. In one step heating (a power jump and about 2.5 min holding), the temperature increases from 2808℃ to 2821℃ and then remains constant for a short time. Thereafter the temperature increases again up to 2825℃. In the next one step heating, the temperature increases without an intermediate holding. The temperature holding is due to the fact that the heat of fusion is additionally required. In the one step cooling, the freezing temperature appears at about 2787℃. We have found that the freezing temperature is quite dependent on the cooling rate and is sometimes not detected. So the freezing temperature was not used for determining the melting temperature.

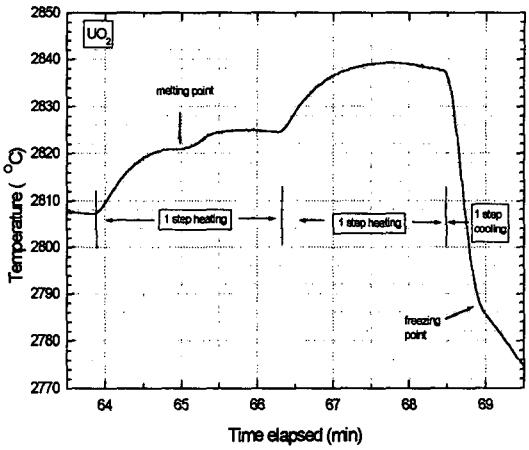

Fig. 3. Temperature-time Plot for UO_2 Melting

We can measure the melting temperature at least 3 times with the same capsule, and the melting point is determined by averaging the three measurements. The melting temperature of UO_2 is 2815±20℃. There are many data about the melting temperature of unirradiated UO_2 determined by the thermal arrest method, and these data are summarized in Table 1 [3-6]. The melting point in our measurement of UO_2, 2815 ±20℃, is in good agreement with the other data.

Fig. 4 shows the cross section of the capsule

Table 1. Comparison of the Melting Temperature of UO_2 with Other Data

References	This work	Hausner [3]	Lyon et al [5]	Latta et al [6]	Tachibana et al [4]
Melting Temperature(℃)	2815 ±20	2805 ±15	2840 ±20	2865 ±15	2845 ±25

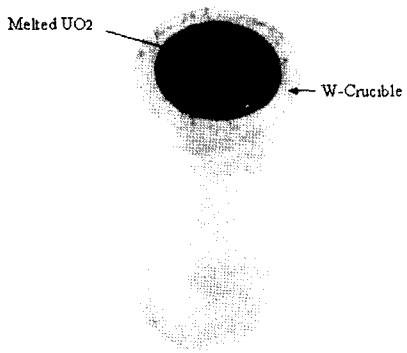

Fig. 4. Tungsten Crucible Containing the Melted UO_2

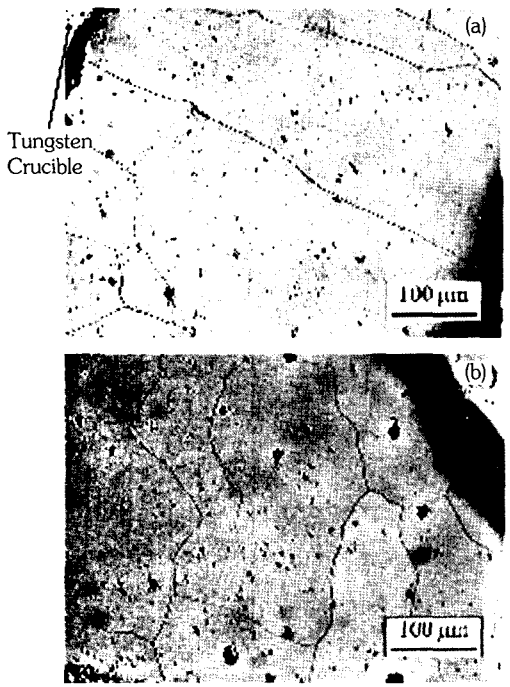

Fig. 5. Microstructure of Melted UO_2; (a) outer region of the capsule, (b) central region of the capsule

containing UO_2 after the melting experiment. Fragments of UO_2 loaded in the capsule were converted to a single body after the experiment, suggesting that the melting has taken place completely.

Fig. 5 shows the grain structure of UO_2 after melting and cooling. It is found that large and columnar grains develop during cooling. Several workers [6,9,14] have reported that some reaction between tungsten capsule and uranium oxide occurred. Latta et al. [6] have reported that the reaction might affect the melting temperature. But Yamanouchi et al. [9] have reported that the reaction did not measurably affect the melting temperature, even if it occurred during heating. Weidenbaum et al. [14] have reported that tungsten dissolves in the melt up to only a few tenths of weight percent. In this work, this kind of tungsten-uranium dioxide reaction was not measurably observed.

4.2. Melting Temperature of $(U,Gd)O_2$

Fig. 6(a) shows a temperature-time profile which indicates that the melting of UO_2-6wt%Gd_2O_3 occurs in one step heating. The solidus and liquidus temperatures are indicated by arrows. The solidus temperature appears broader than the liquidus temperature. The solidus and liquidus temperatures are shown in Table 2.

The temperature-time profile in Fig. 6(b) shows that the melting of UO_2-12wt%Gd_2O_3 occurs in two successive heating steps. We found that the one step heating, which was used for the other fuel materials, could not detect clearly the T_L and

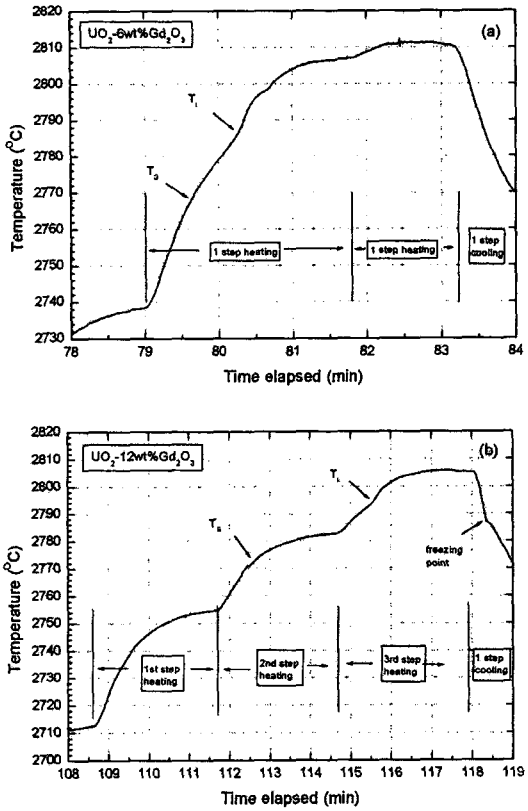

Fig. 6. Temperature-time Plots for UO_2-Gd_2O_3 Fuel Melting. (a) UO_2-6wt%Gd_2O_3 , (b) UO_2-12wt%Gd_2O_3

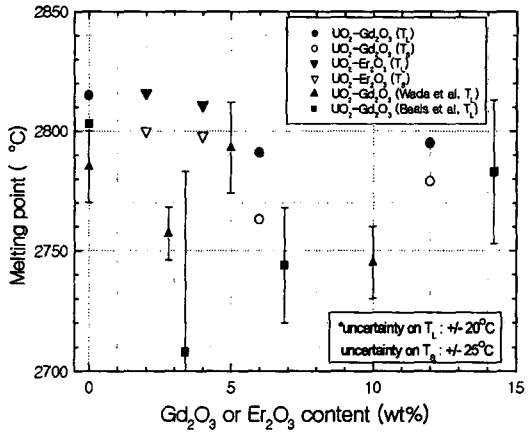

Fig. 7. Melting Temperatures of UO_2, UO_2-Gd_2O_3 and UO_2-Er_2O_3 Fuels

T_S of UO_2-12wt%Gd_2O_3, so such two step heating was tried. The T_L is clearly determined from the point where the rate of temperature rise increases in the third step, and this T_L point is re-identified by the freezing point found in the next cooling step. The T_S can be determined in the following way. The rate of temperature rise at the beginning of the third step is significantly lower than those of two previous steps, suggesting that the melting might start before the third step. We found that the whole temperature rise was smaller in the second step than in the first step, suggesting that the melting start somewhere in the second step. In addition, the rate of temperature rise in the second step seems to slow down significantly at some middle temperature. We assume that this middle temperature in the second step is associated with the T_S. The solidus and liquidus temperatures are shown in Table 2 and plotted in Fig. 7 together with the other liquidus temperatures of Wada et al. [11].

Fig. 7 shows that the liquidus temperatures in our measurement of UO_2-6 and 12wt% Gd_2O_3 are 2790~2795℃ and thus are slightly lower than the UO_2 melting point. The liquidus temperature of Wada et al. [11] decreased with the Gd_2O_3 content, but Beals et al.[10] reported that the T_L was higher at 14wt% Gd_2O_3 than at 7wt% Gd_2O_3. The liquidus temperatures in our measurement of 6wt% and 12wt% Gd_2O_3 are nearly the same. The three experimental results suggest that the T_L decreases with the Gd_2O_3 content in the range of less than about 7wt% Gd_2O_3 but this dependence might be questionable in the large range of Gd_2O_3 content.

Fig. 7 shows that the solidus temperatures of UO_2-Gd_2O_3 are 15~25℃ lower than the liquidus temperatures. Wada et al. did not measure the solidus temperature but have found from some

Table 2. Melting Temperatures of UO_2, UO_2 - Gd_2O_3 and UO_2 -Er_2O_3 fuels

Material	Melting temperature(℃)	
	T_S	T_L
UO_2	2815±20	
UO_2-6wt%Gd_2O_3	2763±25	2791±20
UO_2-12wt%Gd_2O_3	2779±25	2795±20
UO_2-2wt%Er_2O_3	2800±25	2816±20
UO_2-4wt%Er_2O_3	2798±25	2811±20

ceramography experiments that it lies very close to the liquidus temperature. Beals et al. have reported that the solidus temperature is 300~400℃ lower than the liquidus temperature. Our T_S data are in good agreement with the finding of Wada et al.

4.3. Melting Temperature of $(U,Er)O_2$

Fig. 8(a) shows the temperature-time profile which indicates that the melting of UO_2-2wt%Er_2O_3 occurs in one step heating. This temperature profile does not show a clear arrest at a fixed temperature but shows a slow-down in the rate of rising temperature between 2796 and 2814℃. $(U,Er)O_2$ is a solid solution of UO_2 and Er_2O_3 and thus might have both solidus and liquidus temperatures. The start of melting of $(U,Er)O_2$ can be identified by the decrease in the rate of temperature rise, and the end of melting can be identified by the increase in the rate of temperature rise. Solid and liquid are present together between solidus (T_S) and liquidus (T_L) temperatures. In Fig. 8(a), the solidus temperature and liquidus temperature are indicated by the arrows.

The temperature-time profile in Fig. 8(b) shows the melting of UO_2-4wt%Er_2O_3 occurs in one step heating. The temperature profile of Fig. 8(b) is quite similar to that of Fig. 8(a). The solidus and liquidus temperatures are determined by making an average of 3 different measurements and

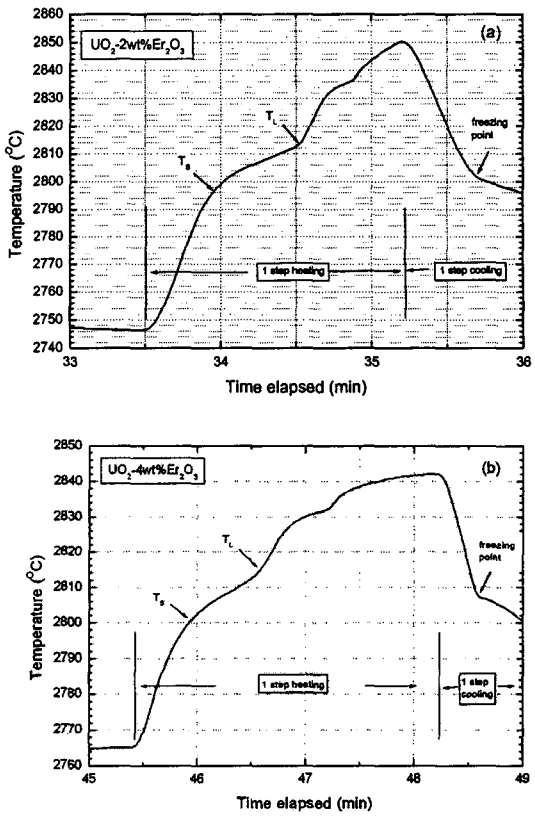

Fig. 8. Temperature-time Plots of UO_2-Er_2O_3 Fuel Melting. (a) UO_2-2wt%Er_2O_3 , (b) UO_2-4wt%Er_2O_3

shown in Table 2.

Fig. 7 shows the liquidus and solidus temperatures of $(U,Er)O_2$. The liquidus temperature decreases very little with the Er_2O_3 content up to 4wt%. The solidus temperature is about 15℃ lower than the liquidus temperature. So the temperature range in which both solid and liquid are present might be very narrow.

5. Conclusions

1) An apparatus was developed for measuring the melting temperature of oxide fuel. This apparatus consists of a high frequency induction furnace, a vacuum chamber, a tungsten capsule,

a pyrometer, a vacuum pump and a data processing system. The melting temperature was determined by the thermal arrest method.

2) The melting temperature of UO_2 is 2815± 20℃. The liquidus temperatures of UO_2-2wt% and 4 wt% Er_2O_3 are very similar to the melting temperature of UO_2, and the solidus temperature is about 15℃ lower than the liquidus temperature.

3) The liquidus temperatures of both UO_2-6wt% Gd_2O_3 and UO_2-12wt% Gd_2O_3 are nearly the same and both are about 20℃ lower than the UO_2 melting temperature. It is found that the solidus temperature is about 25℃ lower than the liquidus temperature.

4) Measured melting temperatures of UO_2, UO_2 - Gd_2O_3 and UO_2 -Er_2O_3 fuels were as follows:

Material	Melting temperature(℃)	
	T_S	T_L
UO_2	2815±20	
UO_2-6wt%Gd_2O_3	2763±25	2791±20
UO_2-12wt%Gd_2O_3	2779±25	2795±20
UO_2-2wt%Er_2O_3	2800±25	2816±20
UO_2-4wt%Er_2O_3	2798±25	2811±20

Acknowledgements

This work has been carried out under the Nuclear R&D Program supported by the Ministry of Science and Technology.

References

1. J. L. Krankota and C. N. Craig, GEAP-13513(1969).
2. J. A. Christensen, Hanford Lab., HW-69234(1962).
3. H. Hausner, J. Nuclear. Mater., 15, 179-183(1965).
4. T. Tachibana, T. Ohmori, S. Yamanouchi and T. Itaki, J. Nucl. Sci. Technol. 22, 155-157 (1985).
5. W. L. Lyon and W. E. Baily, J. Nuclear. Mater., 22, 332-339(1967).
6. R. E. Latta and R. E. Fryxell, J. Nuclear. Mater., 35, 195-210(1970).
7. J. A. Christensen, R. J. Allio and A.Biancheria, WCAP-6065(1965)
8. J. Lambert Bates, J. Nuclear. Mater., 36, 234-236(1970).
9. S. Yamanouchi, T. Tachibana, K. Tsukui and M. Oguma, J. Nucl. Sci. Technol. 25, 528-533(1988).
10. R. J. Beals, J. H. Handwerk and B. J. Wrona, J. Am. Cer. Soc. 52, 578(1969)
11. T. Wada, K. Noro, K. Tsukui, "Behavior of UO_2-Gd_2O_3 fuel," in BNES Nuclear Fuel Performance, (1973).
12. NIST www structural Ceramics Database(Web SCD).
13. M. G. Adamson, E. A. Aitken and R. W. Caputi, J. Nuclear. Mater., 130, 349-365 (1985).
14. B. Weidenbaum and H. Hausner, Trans. Am. Nucl. Soc. 8, 32 (1965).